Title
ELECTRON-CAPTURE AND IMPACT-IONIZATION CROSS SECTIONS FOR PARTIALLY STRIPPED IRON IONS COLLIDING WITH ATOMIC AND MOLECULAR HYDROGEN

Author
Berkner, K.H.

Publication Date
1977-06-01

Submitted to Journal of Physics B

UC-20
LBL-6344 c.1
Preprint

Energy and Environment Division

Electron-Capture And Impact-Ionization Cross Sections For Partially Stripped Iron Ions Colliding With Atomic And Molecular Hydrogen

K. H. Berkner, W.G. Graham, R.V. Pyle,
A.S. Schlachter, J.W. Stearns and R.E. Olson

June 1977

Lawrence Berkeley Laboratory University of California/Berkeley

Prepared for the U.S. Energy Research and Development Administration under Contract No. W-7405-ENG-48

DISCLAIMER

LBL-6344

ELECTRON-CAPTURE AND IMPACT-IONIZATION CROSS SECTIONS FOR PARTIALLY STRIPPED IRON IONS COLLIDING WITH ATOMIC AND MOLECULAR HYDROGEN*

K. H. Berkner, W. G. Graham, R. V. Pyle
A. S. Schlachter, and J. W. Stearns

Lawrence Berkeley Laboratory
University of California
Berkeley, California 94720

and

R. E. Olson

Molecular Physics Center
Stanford Research Institute
Menlo Park, California 94025

June 1977

Abstract

Cross sections for single-electron capture and for impact ionization by Fe^{+q} ($q = 10, 15, 20, 25$) ions incident on atomic hydrogen have been calculated in the energy range 50 to 1200 keV/amu using a classical-trajectory Monte Carlo method. Cross sections for the same processes for Fe^{+q} ions incident on molecular hydrogen have been measured for $q = 11$-22 at 1100 keV/amu, for $q = 9$ at 277 keV/amu, and for $q = 12$ and 14 at 262 keV/amu. The experimental cross sections for molecular hydrogen divided by two are in excellent agreement with the calculated atomic hydrogen cross sections. Scaling laws for the cross sections with q, the charge state of the incident ion, are discussed. The scaling with q is not found to follow the q^2 law predicted by the binary-encounter theory.

*Experimental work done under the auspices of the U.S. ERDA Contract W-7405-ENG-48 and the theoretical work under ERDA Contract E(04-3)-115, P/A No. 111.

1. Introduction

Collision processes involving heavy multicharged ions and H atoms are of both basic and applied interest, especially for the controlled thermonuclear fusion development program. Heavy-ion impurities in a confined plasma can reduce the penetration of energetic neutral deuterium or hydrogen beams injected for heating and fueling the plasma, thus impairing neutral-beam heating of the core of the plasma (Girard et al 1975, Hogan and Howe 1976, Cohen 1976, Barnett 1977). This problem has prompted our interest in the cross sections for the interaction of a D^o beam with heavy, highly ionized impurity ions likely to be found in plasma confinement devices in the energy range of present and future injection schemes, i.e., tens of keV into the MeV region. Heavy impurity ions already observed in present tokamaks include iron and molybdenum ions in charge states as high as +23 for Fe and +31 for Mo (TFR Group 1975 and 1976, Hinnov 1976).

We have chosen to calculate the hydrogen-atom electron-loss cross section for the following two reactions:

$$Fe^{+q} + H \rightarrow \begin{cases} Fe^{+q-1} + H^+ & \text{electron capture} \quad (1) \\ Fe^{+q} + H^+ + e^- & \text{impact ionization} \quad (2) \end{cases}$$

To date, our experimental measurements have been made with hydrogen molecules rather than hydrogen atoms, because of the experimental simplification.

$$Fe^{+q} + H_2 \rightarrow \begin{cases} Fe^{+q-1} + (H_2^+,\ H^+ + H,\ \text{or}\ H^+ + H^+ + e^-) & \text{single electron capture} \quad (3) \\ Fe^{+q} + e^- + (H_2^+,\ H^+ + H\ \text{or}\ H^+ + H^+ + e^-) & \text{impact ionization} \quad (4) \end{cases}$$

For collisions at a sufficiently high energy, a hydrogen molecule can be considered as two hydrogen atoms. This point will be discussed in more detail later in this article. We made the measurements with a fast iron-ion beam incident on a hydrogen target, rather than a fast hydrogen beam incident on an ion target as is the case in a fusion plasma; the cross sections are, of course, the same in either case, when considered in terms of projectile energy per atomic mass unit.

There are very few experimental results for charge transfer of iron ions in H or H_2. Bayfield and his colleagues (Bayfield et al 1977, Gardner et al 1977 a,b) have recently measured the cross sections for electron capture in collisions of Fe^{+q} ions in H and H_2, for $q = 4$-13, in the energy range 27-291 keV/amu. Kim et al (1977) have also measured these cross sections for $q = 6$-8 at 116 keV/amu. The only other charge-transfer measurements for iron ions in H_2 of which we are aware are our recent reports (Berkner et al 1977 a,b) of the charge-transfer cross section for Fe^{+q} in H_2 at 3.4 MeV/amu for $q = 20$-25 and 1.1 MeV/amu for $q = 20$-21. Related measurements, electron-capture cross sections for multicharged C, N, and O projectiles in collisions with atomic or molecular hydrogen, have recently been reported (Olson et al 1977, McKnight et al 1977, Crandall 1976, Crandall et al 1977). We are not aware of previous measurements of impact ionization of H or H_2 by fast highly ionized projectiles.

The only previous theoretical treatment of either electron capture or impact ionization for Fe ions in H or H_2 is the recent work of Olson and Salop (1977), in which both electron-capture and impact-ionization cross sections were calculated for fully-stripped Fe on H from 37.5 keV/amu to 200 keV/amu.

In the present article we report measurements of both single-electron-capture and impact-ionization cross sections for Fe^{+q} in H_2 in the range q = +11 to +22 for an energy of 1.1 MeV/amu, for q = +9 at 277 keV/amu, and for q = +12 and +14 at 262 keV/amu. We used the method of slow-ion and electron collection for the impact-ionization measurements and measurements of the transmitted beam for the charge-transfer determinations. For the theoretical part of this article, the classical-trajectory method was used to calculate both the electron-capture and impact-ionization cross sections for Fe^{+q} in H for q in the range 10-25 at collision energies from 50 keV/amu to 1.2 MeV/amu. Experimental and theoretical results are compared and scaling is discussed.

2. Experimental Approach

2.1 Apparatus

The apparatus is shown in figure 1. Fe^{+16} ions at 62.8 MeV from the SuperHILAC were passed through a 10 μg/cm^2 carbon foil (Foil A in figure 1). Ions of the desired charge state (+11 to +22) were selected by momentum analysis and passed through the target cell described below. The emerging beam was measured by a magnetically suppressed Faraday cup (for impact ionization measurements), or it was momentum analyzed by a spectrometer magnet, and the fast ions in various charge states were detected by an array of five diffused-junction solid-state detectors (for electron-capture measurements). The possible presence of metastable ions in the incident beam is unknown.

For the lower-energy measurements, an Fe^{+9} beam at 15.5 MeV from the SuperHILAC was either used directly or was further stripped in a 10 μg/cm^2 carbon foil to obtain Fe ions in charge states +12 and +14.

The approximate beam energy was obtained from a solid-state detector, and the approximate energy loss in the carbon foil was obtained from Northcliffe and Schilling (1970). The charge state of the beam was then determined to better than two tenths of an electronic charge using a fixed-position, 1.25-mm wide slit in front of a solid state detector in the spectrometer magnet. This system was calibrated both by a wire-orbit measurement and by using a fully stripped carbon-ion beam. Imposing the requirement of integral charge states then allowed us to make a more precise determination of the beam energy. The final energy for the iron-ion beam in the 1.1 MeV/amu experiment was 61.7 ± 0.6 MeV (1.1 MeV/amu); the low energy data for Fe^{+9} incident were at 15.5 ± 0.3 MeV (0.277 MeV/amu), for $Fe^{+12,14}$ at 14.7 ± 0.3 MeV (0.262 MeV/amu).

2.2 Single-electron-capture measurements

The gas cell is a differentially pumped chamber with an inner diameter of 12.1 cm, an entrance aperture 1.5-mm diam (C_3), and an exit aperture 2.23-mm diam (C_4). The incident beam was collimated by a 3.2 mm-diam aperture 178 cm upbeam (C_1 in figure 1). This collimator and the entrance aperture limited the beam size so that essentially no beam was lost at the target exit nor at the Faraday cup or detectors. This was verified by decreasing the exit aperture to 2.00-mm diam for one impact-ionization cross-section measurement. A possible decrease in the cross section of 4% was observed, which was within the experimental uncertainty. The effective beam path length through this target cell was 12.4 cm, assuming a linear pressure drop in the entrance and exit apertures. The pressure in the gas cell was measured with a differential capacitance manometer which was calibrated with an oil manometer. The uncertainty in this measurement is ±4%; combining this with the uncertainty in the gas-cell length and variations in ambient temperature, we estimate ±4% for the target thickness uncertainty.

Apertures C_2 and C_5 (figure 1), 2.5-mm diam, isolated the differential pumped section from the beam line.

Electron-capture measurements were made after first determining that the detected signals for the various charge states were independent of small changes in the spectrometer-magnet field setting. Data were then accumulated in 5 channels for at least 10 different gas-target pressures. Beam attenuation in all cases was less than 15%. The least-squares fit of the $q \rightarrow q-1$ data as a function of target thickness gave $\sigma_{q,q-1}$, with corrections being made for beam attenuation and second-order processes. Typical least squares fits to the data give statistical uncertainties of less than ±4%. The possible systematic errors lead us to believe that the absolute standard error in the cross sections is ±10%.

2.3 Impact-ionization measurements

The impact-ionization cross section was measured by the technique of slow-ion and electron collection. Slow ions and electrons produced by impact ionization or charge transfer were swept from a well-defined length of the target chamber by a variable, weak electric field applied between a pair of 3-cm long plates spaced 1 cm apart and collected on one of these plates. Guard plates were used to provide a uniform electric field in the collection region. The sweeping electric field was increased until the collected currents were insensitive to further changes (75 V/cm). We determined the same cross section using the slow-ion collection data and the electron collection data; the results agreed to within better than 3% (the ion result was higher). This method actually measures the sum of the impact-ionization and electron capture cross sections; however, electron capture is negligible compared to impact ionization at these energies (see table 1). The target gas pressure was measured as in Section 2.2. The estimated uncertainty in the target thickness (molecules/cm^2) is $\pm 4\%$.

Impact-ionization cross sections were determined by measuring simultaneously the slow-ion current in the gas cell and the emerging beam current. Both electrometer signals were integrated for approximately 20 seconds. Measurements were made for at least 10 different gas-cell pressures. The least-squares fit of the ratio of the integrated currents, multiplied by the charge state of the incident ion beam, as a function of target thickness, gave σ_I. Corrections (less than 2%) were made for charge transfer as the beam traversed the target. Typical least squares fits to the data give statistical uncertainties of less than $\pm 1\%$ in most cases. The possible systematic errors lead us to believe that the absolute standard error in the cross section is $\pm 10\%$.

3. Theoretical Approach

The calculations employed in this study are based on the classical-trajectory Monte-Carlo method which has been described in detail in a previous publication (Olson and Salop 1977). This theoretical method has proven to be reliable in predicting the experimental electron-capture and impact-ionization cross sections for $H^+ + H$ collisions (Olson and Salop 1977) and the electron-capture cross sections for the He^{++} + H system (Olson et al 1977) and for collisions of partially stripped C^{+q}, N^{+q} and O^{+q} with H (Olson and Salop 1977, Phaneuf et al 1977). The method is applicable to collisions of heavy, highly-charged ions colliding with a light atom target at collision velocities greater than the orbital velocity of the target atom's electron; for a H-atom target the orbital velocity of the electron is $\sim 2.2 \times 10^8$ cm/sec, which corresponds to ~ 25 keV/amu. A further attribute of the classical trajectory method is that both the electron-capture and impact-ionization cross sections are obtained from the same calculation within the same set of approximations.

Other theoretical methods such as the plane-wave Born approximation (Merzbacher and Lewis 1958), the semiclassical approximation (Bang and Hansteen 1959), and the binary-encounter approximation (Gryzinski 1968, Garcia et al 1968 a,b) are only applicable to light projectile ions such as protons or alpha particles at the collision velocities studied in this paper, and hence cannot be applied to the $Fe^{+q} + H$ systems. However, theoretical methods such as the Glauber (1959) and Magnus (Eichler 1977) approximations should be applicable to the impact-ionization problem. In fact, comparisons between calculated impact-ionization cross sections using the classical-trajectory, Glauber, and Magnus approximations have been made for the He^{++} + H system (Olson et al 1977, Golden and McGuire 1976, Salop and Eichler) and the C^{+6} + H system (Salop and Eichler); the calculations generally agree to within 10-20%.

The classical-trajectory Monte-Carlo method employed in our calculations is based on numerically solving Hamilton's 12-coupled equations of motion for a three-body system (the incident ion, the proton, and the electron initially bound to the proton to form the H-atom target). The equations are solved for a distribution of initial conditions which includes varying the impact parameter and the position and momentum of the electron initially bound by 13.6 eV to the proton. Six random numbers are used to generate the distribution of initial conditions. For each distribution, the classical trajectories of the nuclei are calculated from a large internuclear separation (normally, 10q Bohr radii) to the distance of closest approach and out again to a large internuclear separation. The Coulomb forces between all three bodies are included in the calculation. If, at the end of an individual trajectory, the electron is still bound to the proton, it is catalogued as no reaction. However, if the electron is found bound to the Fe^{+q} projectile ion, it is catalogued as electron capture, and if the electron is bound to neither nucleus, it is catalogued as impact ionization. The cross sections for the various processes are then directly related to the ratio of successful tries for that process to the total number of trajectories calculated.

For the Fe^{+q} + H systems studied, it was normally necessary to calculate 2,000 trajectories at each energy to obtain the electron-capture and impact-ionization cross sections with statistical errors less than 10%. The computer time necessary to calculate the cross sections at one energy scaled directly with q, the charge state of the projectile, and amounted to approximately 0.2 q minutes on a CDC 7600 computer. We should note that once one of the cross sections becomes approximately two orders of magnitude smaller than the other, the statistical uncertainties become very large for the smaller cross section and its value becomes too uncertain to report. Hence, we are unable to estimate the electron-capture cross sections at energies much above 300 keV/amu, since the impact-ionization process strongly dominates the electron loss from the H atom.

4. Results

The calculated cross sections from 50 keV/amu to 1.2 MeV/amu for the Fe^{+q} (q = 10, 15, 20, 25) + H systems are presented in figure 2. Several general features should be noted about the energy dependences of the H-atom electron-loss processes. At collision energies less than $\sim$150 keV/amu, electron capture dominates as the mechanism for electron loss from the H atom. Also, the importance of the electron-capture compared to the impact-ionization process extends to higher collision energies as the charge state of the projectile ion increases. However, as the collision energy is further increased, the electron-capture cross sections decrease precipitately and the impact ionization mechanism dominates the electron loss.

We may compare the theoretical calculations to the experimental cross sections which are given in table 1. For this comparison, however, it is necessary to assume that we may represent the H_2 molecule as two H atoms. This approximation can be assumed to be reasonably valid if we are considering collision energies where an atomic representation is valid. At low collision energies, $E \lesssim 25$ keV/amu, a molecular representation is appropriate and theoretical calculations (Olson and Salop 1976) clearly show that one cannot expect the cross sections for a H_2 target to be two times larger than for an H-atom target. It is difficult to estimate accurately the collision energy above which the atomic representation is valid. However, a reasonable estimate is to use the collision energy at which the electron-capture cross section equals the impact-ionization cross section. From figure 2, we see that this corresponds to 115 keV/amu for Fe^{+10}, 140 keV/amu for Fe^{+15}, 150 keV/amu for Fe^{+20}, and 165 keV/amu for Fe^{+25}. Hence, since our lowest energy for comparison between theory and experiment is 262 keV/amu, we feel reasonably confident that the theoretical cross sections for an H-atom target can be tested against the experimental values for a molecular H_2 target by simply multiplying the cross sections by a factor of two. The scant experimental data available (Olson et al 1977, Gardner et al 1977, McKnight et al 1977) for electron capture of multicharged ions in H and H_2 are not inconsistent with a factor of two for energies above about 150 keV/amu. (They are, however, of insufficient accuracy to permit a more precise conslusion.) There are no previous data for impact ionization.

As our first test, we have compared the experimental and theoretical electron-capture cross sections at 262 keV/amu, figure 3. Experimental measurements were made for $q = 12$ and 14, while theoretical values were calculated for $q = 10, 15, 20$, and 25. The q dependence of the theoretical values is found to be $q^{+2.9 \pm 0.1}$. The magnitude and q dependence of the experimentally measured cross sections are consistent with the theoretical values.

At a higher collision energy, 1.1 MeV/amu, we have been able to determine the q dependence of electron capture cross sections over the range of $q = 12$-22 (figure 4). Only experimental data are presented at this energy since the classical-trajectory calculations are unreliable when the electron-capture cross sections are several orders of magnitude smaller than the impact-ionization cross sections. The q dependence obtained from the data presented on figure 4 is $q^{+3.15 \pm 0.2}$. This increase in the q dependence of the electron-capture cross sections as this collision energy is increased is not inconsistent with other multiply charged ion-atom experimental data that have been analyzed by Nikolaev (1965).

We have also been able to test the calculated impact-ionization cross sections presented in figure 2. At 277 keV/amu, one experimental data point was obtained for $q = 9$. This value is shown compared to the calculated impact-ionization cross sections for $q = 10, 15, 20$, and 25 in figure 5. Tentatively, there appears to be good agreement between theory and experiment, but experimental data for higher q values are needed before the theoretical $q^{+1.40 \pm 0.09}$ dependence is substantiated.

At 1.1 MeV/amu there is a good overlap between the experimental and theoretical cross sections for impact ionization (figure 6). The q dependence, $q^{+1.43 \pm 0.05}$, is found to be almost identical to that obtained at 277 keV/amu.

Hence, predictions of a q^2 dependence for the impact-ionization cross section for a system such as $Fe^{+q} + H$, which are based on an extrapolation of the Born, binary-encounter, or semiclassical approximations, cannot be substantiated.

Acknowledgments

We would like to thank M. I. Green and D. H. Nelson for their advice and assistance in the wire-orbit calibration of the spectrometer magnet, R. R. Stevenson for helpful discussions, and L. A. Biagi, H. H. Hughes, J. R. Meneghetti, and members of their groups for skillful technical assistance.

References

Bang J and Hansteen J M 1959 *Kgl. Danske Vidensk.* 31 No. 13.

Barnett C F 1977 *Atomic Physics 5*, R Marrus, M Prior and H Shugart, eds. (New York: Plenum Press) 375-90.

Bayfield J E, Gardner L D, Kin H J and Stelson P H 1977 *Bull. Am. Phys. Soc.* 22 83.

Berkner K H, Graham W G, Pyle R V, Schlachter A S and Stearns J W 1977a submitted to *Phys. Lett. A*.

_____ 1977b *Abstr. Xth ICPEAC* (Paris).

Cohen S A 1976 *J. Vac. Sci. Technol.* 13 449-62.

Crandall D H 1976 *Proc. Fourth Conf. on Scientific and Industrial Applications of Small Accelerators* Rept. 76Ch 1175-9 NPS, p 157.

Crandall D H, Mallory M L and Kocher D C 1977 *Phys. Rev. A* 15 61-9.

Eichler J 1977 *Phys Rev. A* 15 1856-62.

Garcia J D, Gerjuoy E and Welker J E 1968a *Phys. Rev.* 165 66-72.

_____ 1968b *Phys. Rev.* 165 72-80.

Gardner L D and Bayfield J E 1977, Private Communication.

Gardner L D, Bayfield J E, Koch P M, Kim H J, and Stelson P H 1977a, to be published in *Phys. Rev. A*.

_____ 1977b *Bull. Am. Phys. Soc.* 22 83.

Girard J P, Marty D A and Moriette P 1975 *Plasma Physics and Controlled Nuclear Fusion Research* (Vienna: IAEA) IAEA-CN-33/A 17, pp 681-96.

Glauber R J 1959 *Lectures in Theoretical Physics*, W E Brittin, ed. (New York: Interscience) Vol. I, p 315.

Golden J E and McGuire J H 1976 *J. Phys. B: Atom. Molec. Phys.* 90 L11-L13.

Gryzinski M 1965 *Phys. Rev.* A336-A358

Hinnov E 1976 *Phys. Rev. A* 14 1533-41.

Hogan J T and Howe H C 1976 *J. Nucl. Mater.* 63 151-57.

Kim H J, Meyer F W and Phaneuf R A 1977 unpublished.

Merzbacher E and Lewis W H 1958 *Handbuch der Physik*, S Flugge, ed. (Berlin: Springer) Vol. 34, p 166.

McKnight R H, Phaneuf R A and Meyer F W 1977 submitted to *Phys. Rev. A.*

Nikolaev V S 1965 *Sov. Phys.-Uspekhi* 8 269-94.

Northcliffe L C and Schilling R F 1970 *Nucl. Data Tables* A7 233-2.

Olson R E and Salop A 1977 *Phys. Rev. A* 16 (Aug.).

_____ 1976 *Phys. Rev. A* 14 579-85

Olson R E, Salop A, Phaneuf R A and Meyer F W 1977 *Phys. Rev. A* 16 (in press).

Phaneuf R A, Meyer R A, McKnight R H, Olson R E, and Salop A 1977 *J. Phys. B: Atom. Molec. Phys.* 9 (in press).

Salop A and Eichler J, Private Communication.

TFR Group 1976 *J. Nucl. Mater.* 63 47-58.

TFR Group 1975 *Nucl. Fusion* 15 1053-66.

Table 1. Experimental single-electron-capture cross sections ($\sigma_{q,q-1}$) and impact-ionization cross sections (σ_I) for Fe^{+q} +H_2 collisions. All cross sections have an absolute uncertainty of ±10% except for the one marked a, for which the uncertainty is ±15%.

Energy (MeV/amu)	Incident charge state, q	Cross sections ($10^{-17} cm^2$/molecule)	
		$\sigma_{q,q-1}$	σ_I
1.10	+11		330
	+12	0.064[a]	355
	+13		385
	+14	0.109	435
	+16	0.142	510
	+18	0.250	630
	+20	0.315	740
	+22	0.430	950
0.277	+9	11.9	485
0.262	+12	32.8	
	+14	57.0	

Figure Legends

Figure 1 Schematic diagram of the apparatus. Dimensions for collimators C_1-C_5 are in the text. Foil B was used only for calibration of the spectrometer magnet.

Figure 2 Calculated cross sections for Fe^{+q} (q = 10, 15, 20, 25) + H collisions. The open squares denote the single-electron-capture cross section, the open triangles the impact-ionization cross section, and the open circles the total cross section for electron loss by the H atom.

Figure 3 Calculated single-electron-capture cross sections for Fe^{+q} (q = 10, 15, 20, 25) + H collisions at 262 keV/amu (open squares, right ordinate), and experimental single-electron-capture cross sections for Fe^{+q} (q - 12, 14) + H_2 collisions at 262 keV/amu (closed squares, left ordinate). The line shown is a fit of the calculated cross sections to a function $\sigma = \sigma_1 q^{\alpha}$, where $\alpha = 2.9 \pm 0.1$ and $\sigma_1 = 1.1 \pm 0.05 \times 10^{-19}$. Statistical uncertainties in the calculated cross sections are ±15%.

Figure 4 Experimental single-electron-capture cross sections for Fe^{+q} (q = 12-22) + H_2 collisions at 1.1 MeV/amu. The dotted line shows a least-squares fit of the cross sections to a function $\sigma = \sigma_1 q^{\alpha}$, where $\alpha = 3.15 \pm 0.2$ and $\sigma_1 = (2.6 \pm 0.2) \times 10^{-22}$.

Figure 5 Calculated impact-ionization cross sections for Fe^{+q} (q = 10, 15, 20, 25) + H collisions at 277 keV/amu (open triangles, right ordinate) and experimental impact-ionization cross sections for $Fe^{+9} + H_2$ collision at 277 keV/amu (closed triangle, left ordinate). The line shows a least-squares fit of the calculated cross sections to a function $\sigma = \sigma_1 q^{\alpha}$, where $\alpha = 1.40 \pm 0.09$ and $\sigma_1 = (1.08 \pm 0.05) \times 10^{-16}$. Statistical uncertainties in the calculated cross sections are $\pm$ 5%.

Figure 6 Calculated impact-ionization cross sections for Fe^{+q} (q = 10, 15, 20, 25) + H collisions at 1.1 MeV/amu (open triangles, right ordinate) and experimental impact-ionization cross sections for Fe^{+q} (q = 11-22) + H_2 collisions at 1.1 MeV/amu (closed triangles, left ordinate). The dotted line shows a least-squares fit of the experimental cross sections to a function $\sigma = \sigma_1 q^{\alpha}$, where $\alpha = 1.43 \pm 0.05$ and $\sigma_1 = (9.9 \pm 0.2) \times 10^{-17}$. Statistical uncertainties in the calculated cross sections are $\pm$ 5%.

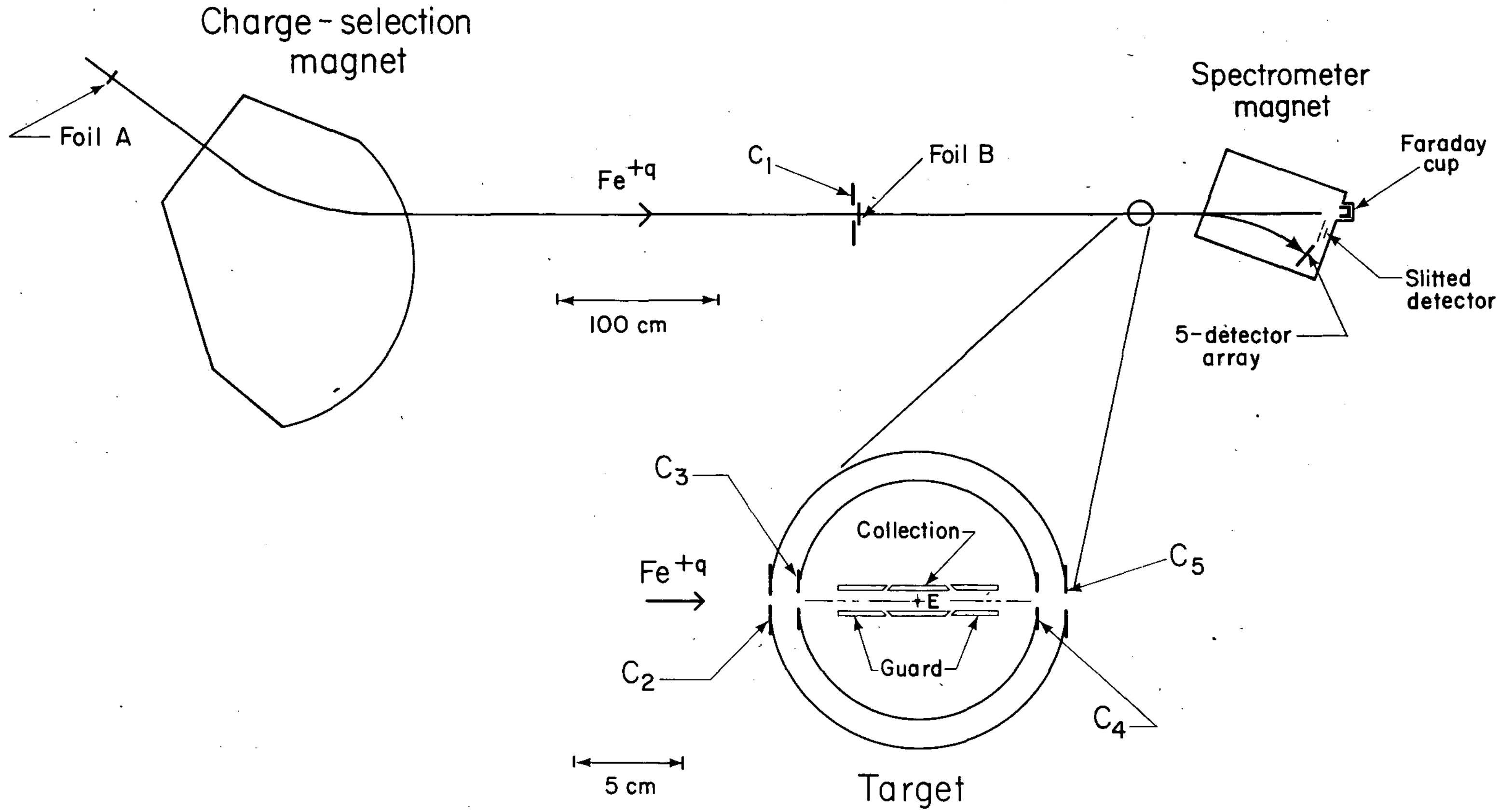

XBL 776-1127

Fig. 1

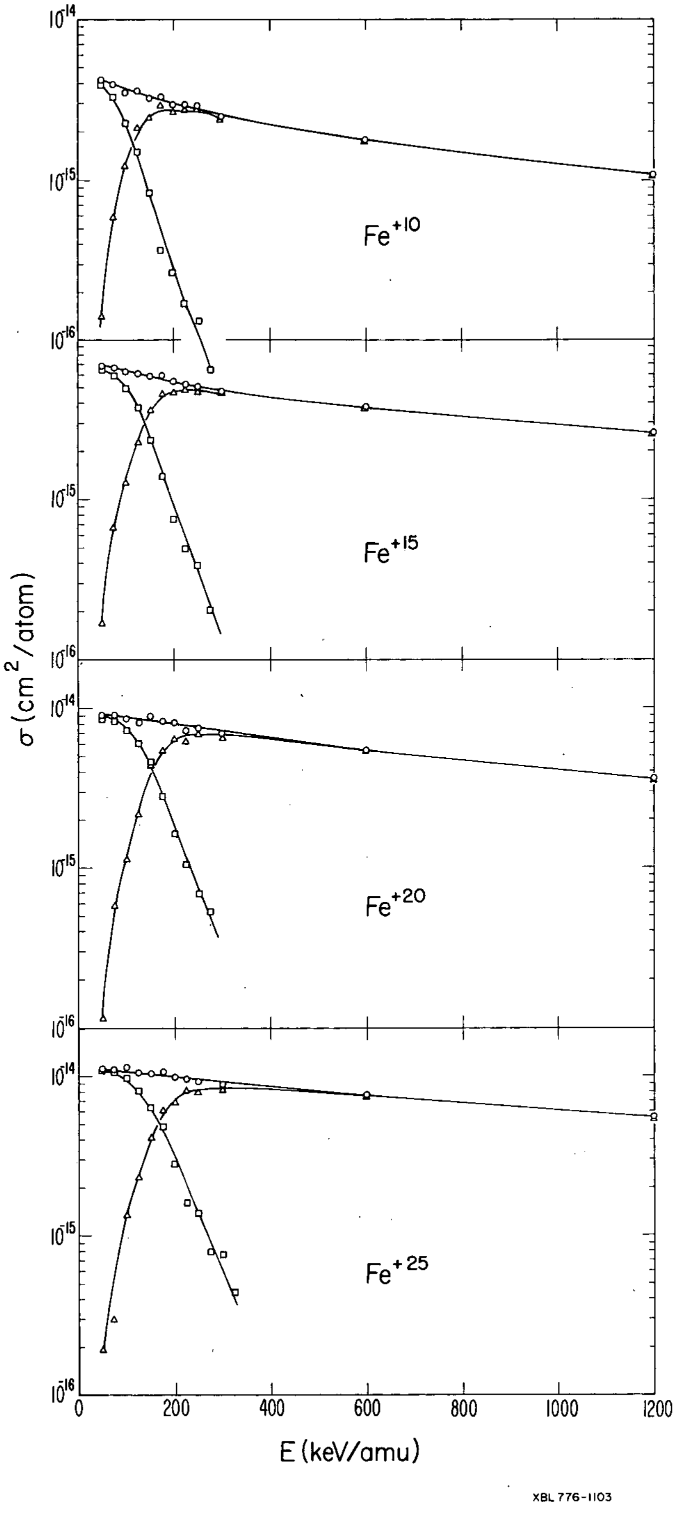

10^{-14}
10^{-15}
10^{-16}
Fe+10
Fe+15
Fe+20
Fe+25
σ (cm² /atom)
0
200
400
600
800
1000
1200
E (keV/amu)
XBL 776-1103

Fig. 2

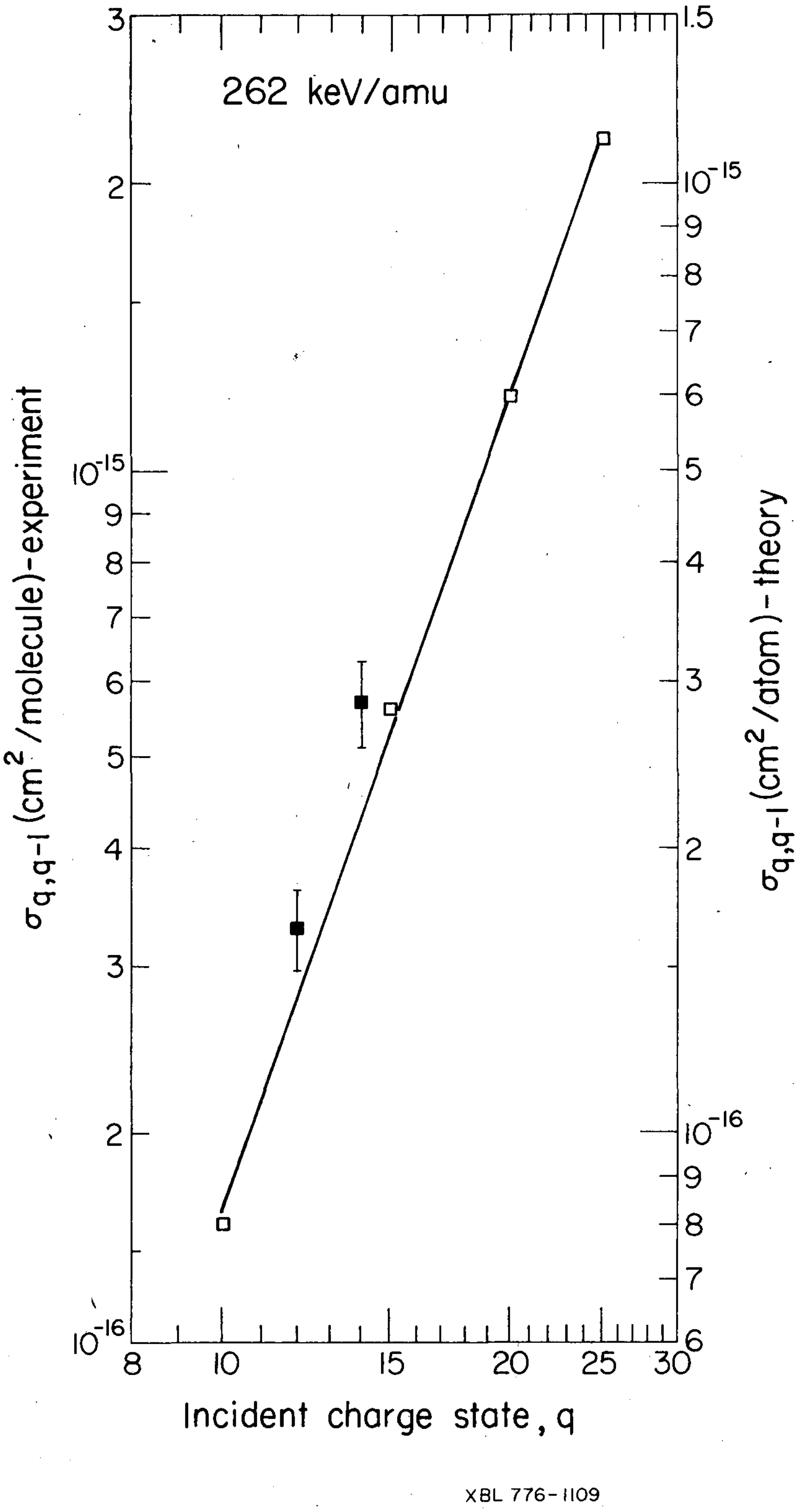
262 keV/amu
$\sigma_{q,q-1}$ (cm^2/molecule)-experiment
$\sigma_{q,q-1}$(cm^2/atom)-theory
Incident charge state, q
3
2
10^{-15}
9
8
7
6
5
4
3
2
10^{-16}
1.5
10^{-15}
9
8
7
6
5
4
3
2
10^{-16}
9
8
7
6
8
10
15
20
25
30
XBL 776-1109

Fig. 3

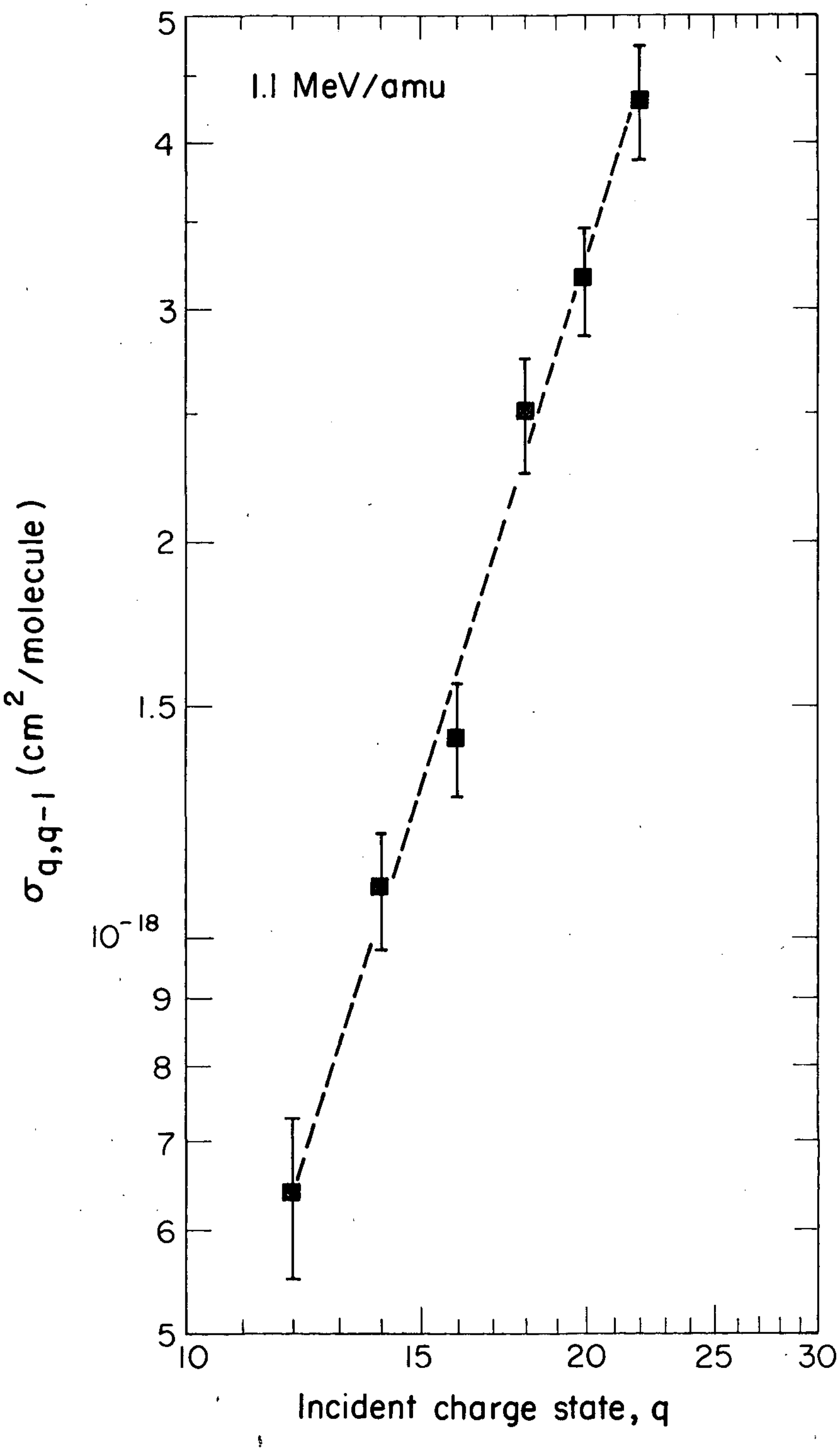

XBL 776-1106

Fig. 4

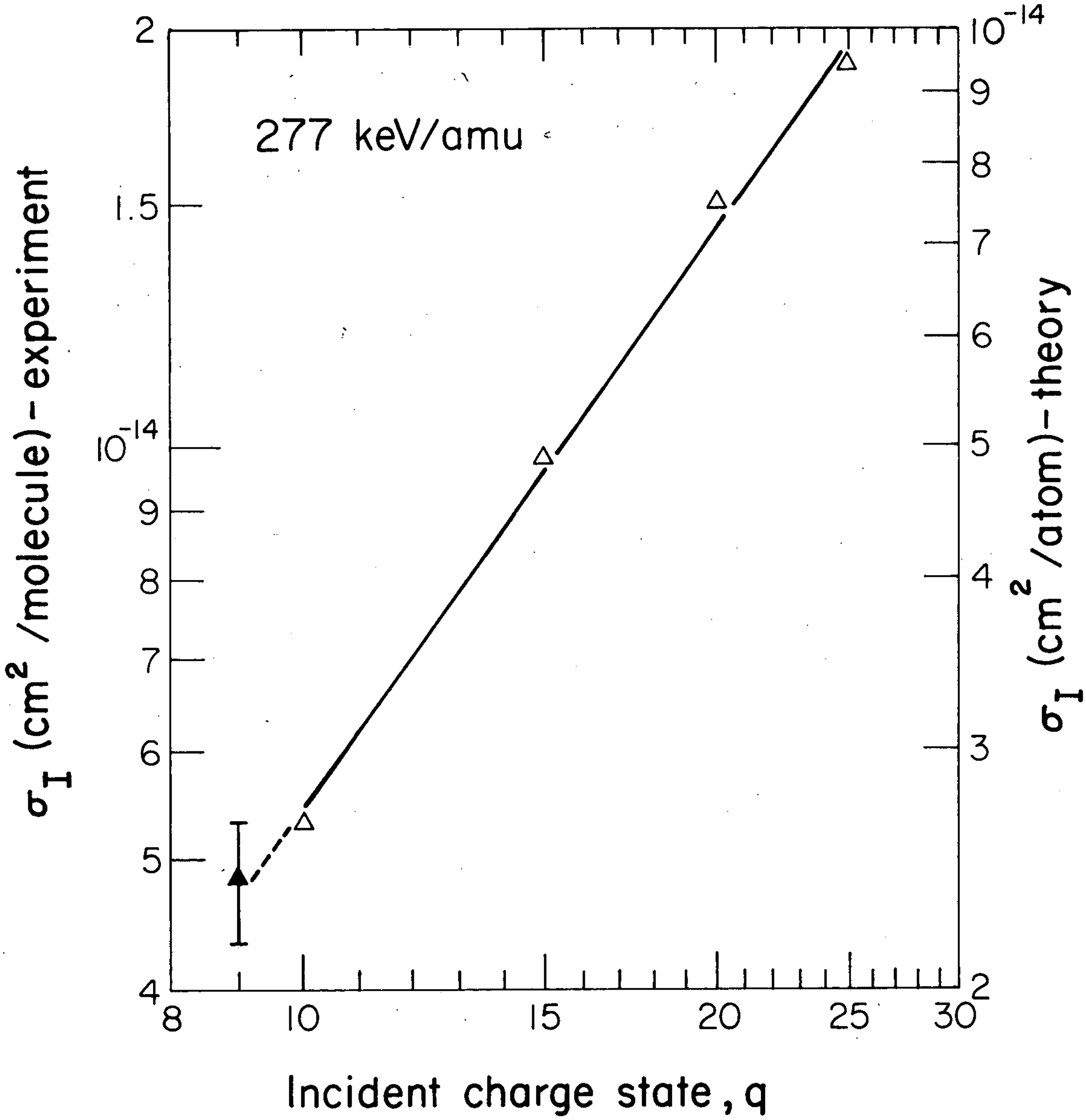
277 keV/amu
σ_I (cm^2 /molecule) - experiment
σ_I (cm^2 /atom) - theory
Incident charge state, q
2
1.5
10^{-14}
9
8
7
6
5
4
8
10
15
20
25
30
XBL 776-1111

Fig. 5

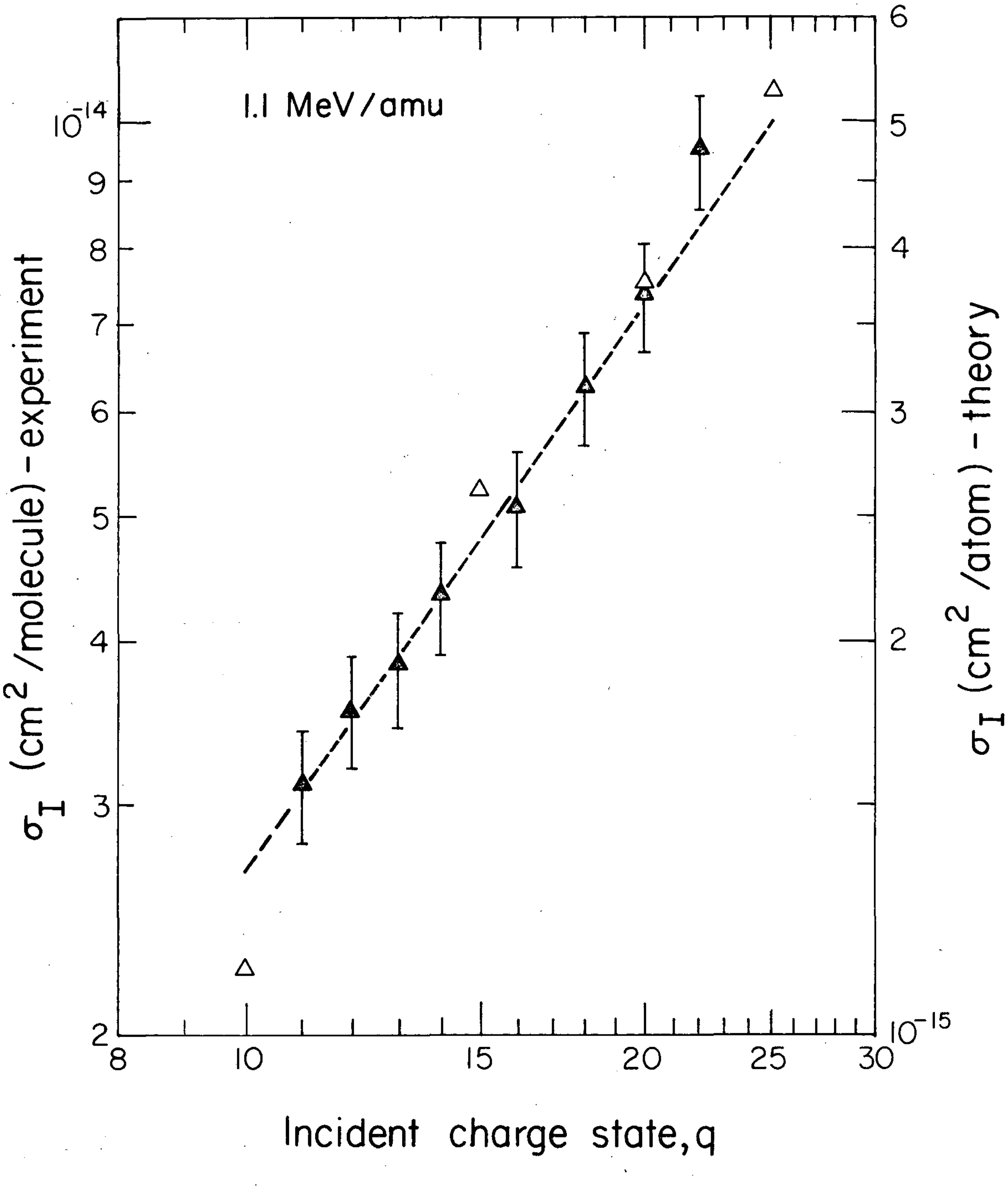
1.1 MeV/amu
10^{-14}
9
8
7
6
5
4
3
2
6
5
4
3
2
10^{-15}
8
10
15
20
25
30
σ_I (cm^2/molecule) - experiment
σ_I (cm^2/atom) - theory
Incident charge state, q
XBL 776-1110

Fig. 6

TECHNICAL INFORMATION DEPARTMENT
LAWRENCE BERKELEY LABORATORY
UNIVERSITY OF CALIFORNIA
BERKELEY, CALIFORNIA 94720